

Isospin influence on the decay modes of compound systems produced in the $^{78,86}\text{Kr} + ^{40,48}\text{Ca}$ at 10 AMeV

S. Pirrone¹, G. Politi^{1,2}, J.P. Wieleczko⁵, E. De Filippo¹, B. Gnoffo¹, P. Russotto^{1,2}, M. Trimarchi^{7,8}, M. La Commara^{3,4}, M. Vigilante^{3,4}, G. Ademard¹¹, F. Amorini⁶, L. Auditore^{7,8}, C. Beck⁹, I. Berceanu¹⁰, E. Bonnet⁵, B. Borderie¹¹, G. Cardella¹, A. Chibih⁵, M. Colonna⁶, A. D'Onofrio^{4,12}, J. D. Frankland⁵, E. Geraci^{1,2}, E. Henry¹³, E. La Guidara^{1,14}, G. Lanzalone^{6,15}, P. Lantesse¹⁶, D. Lebhertz⁵, N. Le Neindre¹⁷, I. Lombardo^{3,4}, K. Mazurek⁵, S. Norella^{7,8}, A. Pagano¹, E.V. Pagano^{2,6}, M. Papa¹, E. Piasecki¹⁸, F. Porto^{2,6}, L. Quattrocchi^{7,8}, M. Quinlann¹³, F. Rizzo^{1,6}, W. U. Schroeder¹³, G. Spadaccini^{3,4}, A. Trifirò^{7,8}, J. Toke¹³ and G. Verde^{1,11}

¹INFN Sezione di Catania, Italy

²Dipartimento di Fisica e Astronomia, Università di Catania, Italy

³Dipartimento di Fisica, Università Federico II Napoli, Italy

⁴INFN Sezione di Napoli, Italy

⁵GANIL Caen, France

⁶INFN Laboratori Nazionali del Sud, Italy

⁷Dipartimento di Fisica, Università di Messina, Italy

⁸INFN Gruppo collegato di Messina, Italy

⁹IN2P3 - IPHC Strasbourg, France

¹⁰IPNE, Bucharest, Romania

¹¹IN2P3 - IPN Orsay, France

¹²Dipartimento di Matematica e Fisica - Seconda Università di Napoli, Caserta, Italy

¹³University of Rochester, USA

¹⁴Centro Siciliano Fisica Nucleare e Struttura della Materia, Catania, Italy

¹⁵Università Kore, Enna, Italy

¹⁶IN2P3 - IPN Lyon, France

¹⁷IN2P3 - LPC Caen, France

¹⁸University of Warsaw, Poland

Abstract. The study of the decay modes competition of the compound systems produced in the collisions $^{78}\text{Kr}+^{40}\text{Ca}$ and $^{86}\text{Kr}+^{48}\text{Ca}$ at 10 AMeV is presented. In particular, the N/Z entrance channel influence on the decay paths of the compound systems, directly connected to the isospin influence, is investigated. The experiment was performed at the INFN Laboratori Nazionali del Sud (LNS) in Catania by using the 4π multi-detector CHIMERA. Charge, mass, angular distributions and kinematical features of the reaction products were studied. The analysis shows some differences in the contribution arising from the various reaction mechanisms for the neutron poor and neutron rich systems. Comparison with theoretical statistical and dynamical models are presented for the two systems. Besides a study of the influence of the energy on the entrance channel is performed for the $^{78}\text{Kr}+^{40}\text{Ca}$ reaction, by comparing the results of this experiment to those obtained for the same system at 5.5 AMeV with the INDRA device at GANIL.

¹ Corresponding author: sara.pirrone@ct.infn.it

1 Introduction

One of the principal aim in the field of the nuclear reactions is the study of the influence of the entrance channel N/Z ratio, directly connected to the isospin degree of freedom, on the reaction mechanism and on the formation of the fragments in the exit channel.

In this context, particular interest is focused on the heavy-ion reactions at low energy ($E/A < 10-15$ AMeV), where for medium-mass systems the fusion processes are predominant. Indeed, one expects that the N/Z ratio of the compound nucleus, plays an important role on its decay evaporation-process, providing crucial information on fundamental nuclear parameters as the level density, the fission barrier and the nuclear viscosity. Thus a program of detailed measurements of reaction cross-section for a large isotopic chain of compound nuclei, from neutron rich to neutron-poor, can provides careful information.

In this work, we present the up to date results of the ISODEC experiment, realized to study the competition among the various disintegration modes of $^{118,134}\text{Ba}$ compound nuclei produced in the reactions $^{78}\text{Kr}+^{40}\text{Ca}$ (neutron poor system) and $^{86}\text{Kr}+^{48}\text{Ca}$ (neutron rich system) at 10 AMeV. The experiment was performed at the INFN Laboratori Nazionali del Sud (LNS) in Catania by using the CHIMERA detector. It complements and improves the data obtained at 5.5 MeV/A for $^{78,82}\text{Kr}+^{40}\text{Ca}$ reactions [1], previously realized with beams delivered by GANIL facility and by using the INDRA detector.

The two investigated systems are different for 16 neutrons, the maximum difference that we can get by using stable nuclei; this allows to produce compound nuclei with similar both spin distribution and excitation energy in a large domain of N/Z (from 1.11 to 1.39). Such a set of data also will provide new constraint on sophisticated models attempting to describe statistical and/or dynamical properties [2] of excited nuclei.

2 Experimental set-up

In order to realize the presented scientific program, we need the measurements of several key observables such as the cross sections, multiplicities, angular and kinetic energy distributions of the various reaction products: Intermediate Mass Fragments - IMFs, Light Charge Particles - LCPs, Evaporation Residues - ER, and Fission Fragments - FF. The measurement of these observables requires a good isotopic resolution, a low energy thresholds for LCPs and IMFs, an high angular resolution and a broad angular acceptance.

The presence at LNS of CHIMERA [3], a second generation 4π multi detector, and the possibility to get beams with both good intensity and timing characteristics, strongly supported the necessity to perform the experiment in Catania.



Figure 1. CHIMERA in the scattering chamber at INFN-LNS

CHIMERA consists of 1192 detector telescopes, arranged on 9 rings in the forward part, that cover a polar angle from 1° to 30° , and 17 rings in spherical configuration, that cover from 30° to 176° . The geometrical efficiency is the 94% of the total solid angle. In figure 1, a picture of the detector in its own experimental scattering chamber at LNS is presented.

The single detection telescope consists of a silicon detector (Si, thickness about $300\ \mu\text{m}$) followed by a Caesium Iodine Thallium doped crystal, (CsI(Tl), thickness from 3 cm to 12 cm), coupled to a photodiode.

The identification methods employed are:

$\Delta E-E$ for charge identification of particles punching through the Si detector and stopped in the CsI(Tl) with also mass identification for particles with $Z < 10$;

E-TOF (Time of Flight) for mass identification, velocity and energy measurement of the particles stopped in the Si detector;

PSD (Pulse Shape Discrimination) in CsI(Tl), for isotopic identification of more energetic light charge particles;

PSD (Pulse Shape Discrimination) in Si detector, for charge identification of the particles stopped in the Silicon detector.

Besides, the CHIMERA multi detector is characterized by a low energetic detection threshold, that is less of 0,5 MeV/A for heavy ions and about 1 MeV/A for light particles.

Concerning the PSD in silicon detector [4, 5, 6], this was the last implementation made on the CHIMERA array and allows the use of this device to study reaction mechanism also in the low energy domain, extending the investigation dynamical range of the detector from the fusion to the multi fragmentation reactions.

In the experiment, self-supporting 1 mg/cm² thick ⁴⁰Ca and ⁴⁸Ca targets, prepared in collaboration between INFN-LNL and INFN-LNS Target Laboratories, were bombarded by ^{78,86}Kr beams at 10 AMeV, delivered by the LNS Superconductive Cyclotron, with typical beam current intensity of 800-1000 pA. The pulsed beam was delivered with a timing resolution in the range 800 ps - 1 ns. Inclusive and coincidence measurements were realized.

In figure 2 is reported as an example the Energy (E_{Si}) vs Rise Time (RT_{Si}) plot obtained by the PSD methods in silicon detector, for the n-poor system ⁷⁸Kr+⁴⁰Ca at 10 AMeV at $\theta=34^\circ$. Identification energy threshold of about 4.5 MeV/nucleon was obtained. Notice that in CHIMERA PSD identification of fragment are obtained mounting the silicon detectors in direct mode in order to allow good timing performances needed for the TOF identification.

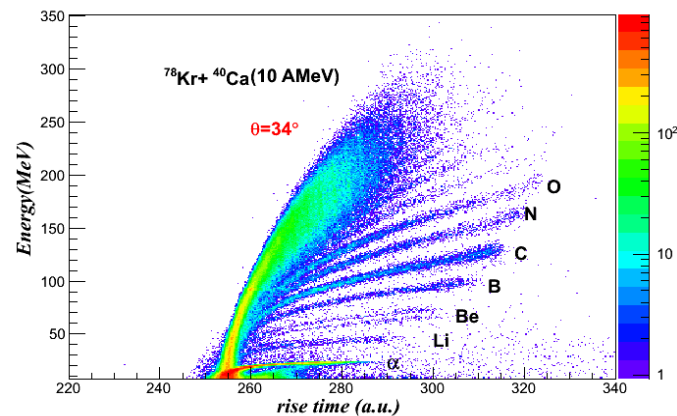


Figure 2. Energy-RiseTime plot for ⁷⁸Kr+⁴⁰Ca

These characteristics allowed the complete identification of LCP in a wide energy range, the complete identification in charge and mass of the IMF ($3 < Z < 8$) products, the charge identification up to $Z = 14-17$ for fragments stopped in the Silicon, and up to about $Z = 30$ for the most energetic particles stopped in CsI.

In figure 3 is reported an example of typical matrix ΔE -E that shows the good identification capability of the array. We see a very good discrimination in charge and also in mass for the lighter nuclei, up to Carbon.

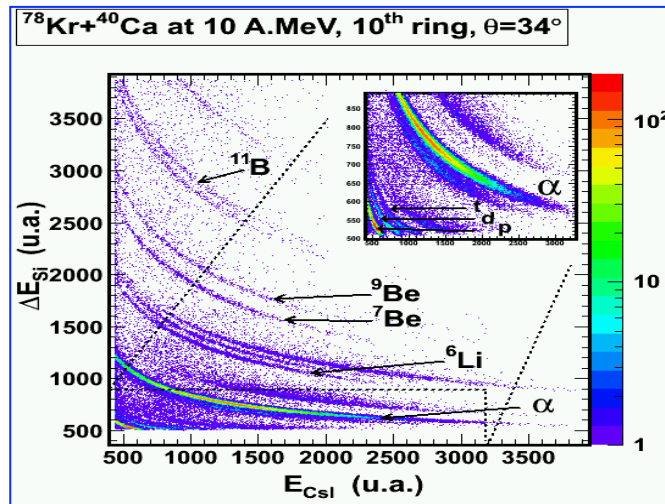


Figure 3. $\Delta E_{Si}-E_{CsI(TI)}$ plot for $^{78}\text{Kr}+^{40}\text{Ca}$

In particular, in figure 4 is reported an example of isotopic identification for Carbon isotopes obtained at polar angle of 15° for the two systems [6].

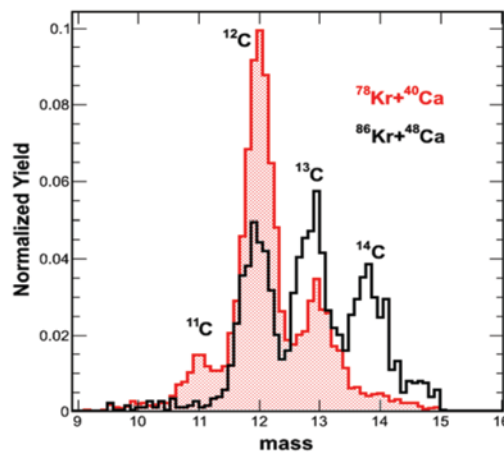


Figure 4. Carbon isotopes distributions at 15° for the two systems

3 Experimental Results

3.1 Mass distribution

In order to study the influence of the isospin degree of freedom it is essential to get the isotopic identification at least of part of the detected fragments. The capability of the CHIMERA detector allows us to get the mass distributions for the IMF $2 \leq Z \leq 8$.

In figure 5 the mass distribution for $Z = 3, 4, 5$ and for the two studied systems are reported.

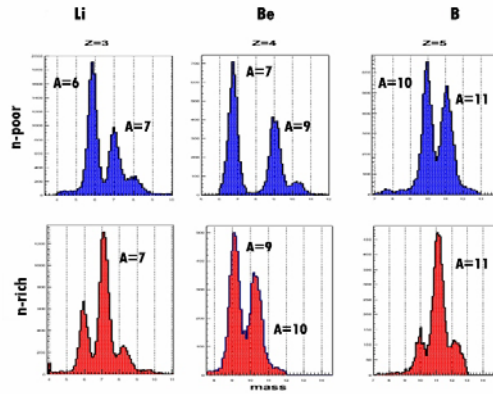


Figure 5. Mass distributions for $Z=3,4,5$, for the n-poor system and n rich system

One can see the different isotopic composition and relative enrichment in correspondence of the same Z , for the compared systems. In particular this effect is evident for the Be element, in which the isotopic composition goes from $A=7, 9$, in the n-poor system, to $A= 9,10$, in the n-rich one. These differences in the two systems show that a memory of the entrance channel is still present in this class of reaction products, and it could be due to an effect of the isospin influence on the reaction mechanism or, alternatively, on the structure of the emitted fragments.

3.2 Charge distribution

The influence of the isospin on the reaction mechanism and on the fragments production should appear also in the charge distribution.

A comparison between the fragments yields as a function of their charge for the studied systems is presented in Figure 6. The IMF cross section behaviour exhibits for both systems a strong even-odd effect, the staggering, due to a preferential production of fragments with even value of the atomic number. In agreement with other examples in literature [1, 8, 9] the staggering is more pronounced for the n-poor system respect to the n-rich one, in particular for $Z<10$ reaction products as it is shown in figure 6. This effect persists for higher Z , but with a smaller amplitude.

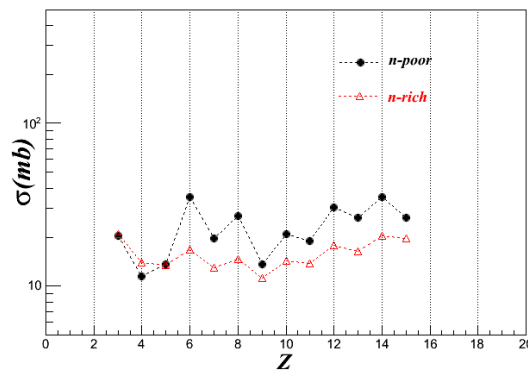


Figure 6: IMF Charge distributions, in red triangle for the $^{86}\text{Kr}+^{48}\text{Ca}$ reaction, in black circle for the $^{78}\text{Kr}+^{40}\text{Ca}$ reaction (color on line)

It seems that the neutron excess in the entrance channel affects the yields of the light fragments. An Influence can be originated also by structure effects [10] linked to the pairing forces, and it could be connected with the Symmetry Energy.

The charge distributions of the two systems were compared with the preliminary results of model calculations. In order to understand the origin of the different behaviour, we performed calculations with the dynamical DNS (Di Nuclear System) model for $Z<10$, and with the GEMINI ++ code, a Montecarlo Code basing on recent statistical model, for Z up to 16 .

Following the dynamical DNS (Di Nuclear System) model, a dinuclear system is formed in the beginning of the reaction, that can go towards a not fully equilibrated fast-fission or towards an equilibrated fissioning compound nucleus. A detailed description of the model can be found in [11,12].

The simulation of GEMINI++ code reproduces the decay of the compound nucleus following the formalism of the Hauser-Feshbach [13], taking in account the probability of asymmetric fission obtained by L. Moretto in an extension of the transitional state model [14,15].

The results of these comparisons are reported in figure 7.

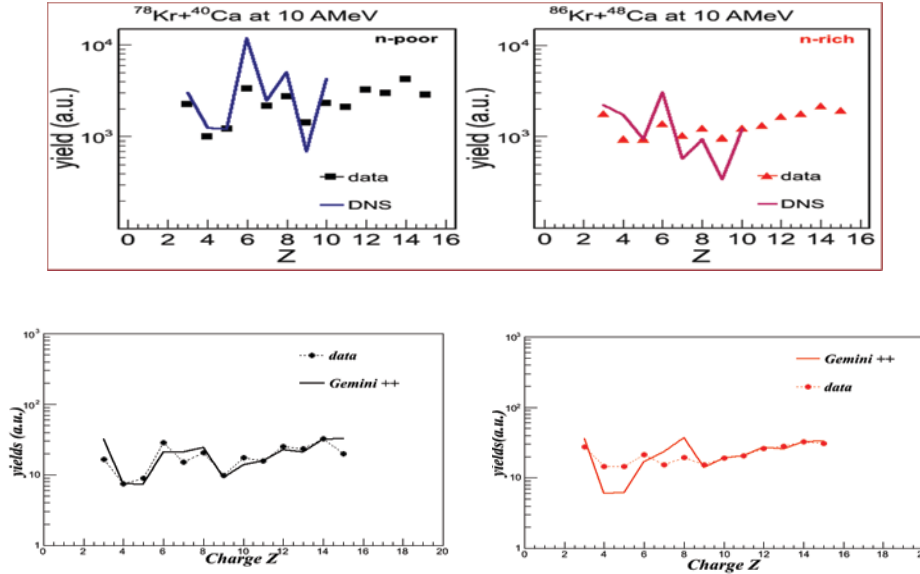


Figure7: top, comparison with DSN model; bottom, comparison with GEMINI++ model

The calculations seem to be in a slightly better agreement in the case of the neutron poor system in both cases. This behaviour could be the indication that the n-enrichment could favour new mechanism in the production of intermediate mass fragments, not considered in the used models, neither dynamics or statistical.

In both systems, for higher Z, the oscillation of the staggering of the yields is decreasing as the atomic number increases in agreement with the experimental findings.

3.3 Kinematical features

The good measurement of time of flight of the reaction products, allows to us to calculate the average velocity in the centre of mass $\langle v_{cm} \rangle$ for Z from 3 to 17. The results are reported in Figure 8 at various laboratory angles for the neutron poor system. We note that for a given Z the average velocity in the centre of mass is constant within the experimental accuracy with respect to the emission angle.

This general behaviour observed for the emitted fragments, give us an indication of the high degree of relaxation in the production mechanism.

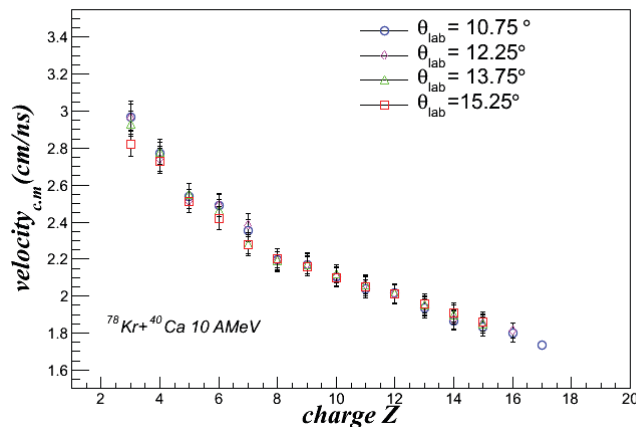


Figure 8. Average velocity distribution

As shown in figure 9, we also note that the mean values of the velocity of the IMF in the centre of mass frame show a quasi-linear decrease with the increase of the atomic number and they are well reproduced by the prediction of the fission systematic of Viola, with the Hinde's correction for the asymmetric process [16].

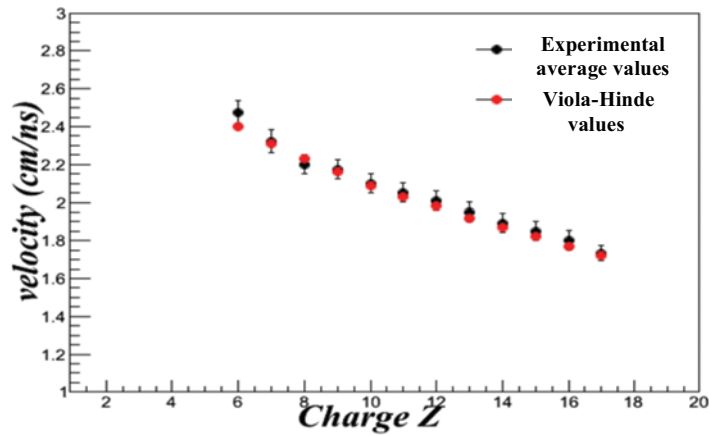


Figure 9 : Comparison of the mean values of the velocity, averaged over all angles, with the values of Viola, for the reaction $^{78}\text{Kr}+^{40}\text{Ca}$

3.4 Angular distribution

The study of the angular distribution of the emitted fragments allows us to get fundamental information to distinguish totally equilibrated processes, as the compound nucleus formation followed by evaporation or fission, from partially equilibrated process as the fast-fission or the DIC processes.

Some examples are given in the following. In figure 10, the angular distributions of fragments with Z from 12 to 32, for the neutron poor system, are compared to the $1/\sin\theta$ behaviour (dashed line), that is the behaviour of the isotropic emission typical of the fission fragments (FF) coming a fissioning compound nucleus.

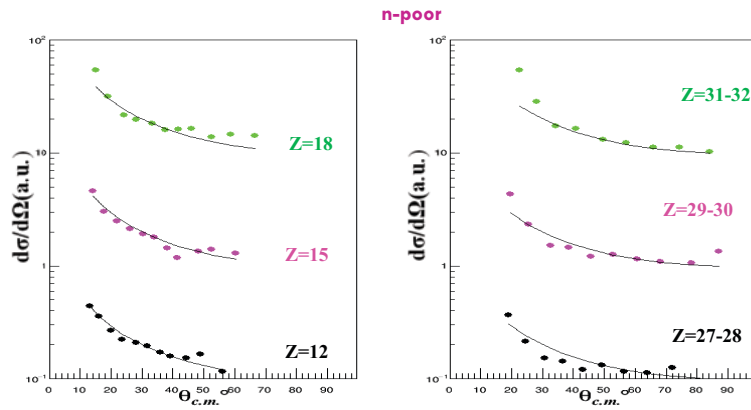


Figure 10 For the $^{78}\text{Kr}+^{40}\text{Ca}$ reaction. FFs angular distributions, in the center of mass frame, the solid line is $1/\sin\theta_{cm}$

Besides, if we look at the angular distributions of the heavier reaction products in the laboratory frame; shown in figure 11, we see that they are very strongly forward peaked, as it is expected in the case of evaporation residue, (ER)

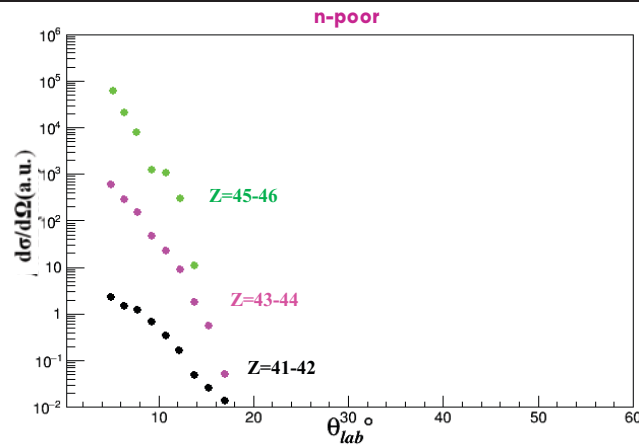


Figure 11 For the $^{78}\text{Kr}+^{40}\text{Ca}$ reaction. ER angular distributions, in the laboratory frame

Finally, starting from angular distributions for the different selected reaction products, with a suitable normalization, we obtain the cross sections for the different reaction mechanisms.

3.5 Global features

In order to investigate about the global features of the reactions complete events were selected by imposing the conditions of total detected mass $M_{tot} > 90$ and total momentum $P_{tot} > 0.7P_{beam}$ [17,18]. By looking at the plot of the mass versus the parallel velocity for each reaction product, reported in figure 12, we can extract qualitative information about the competition among the different decay channels. In fact in this plot the different reaction products, coming by the Fusion-Fission and Quasi-Fission decay process or by Evaporation Residues one, can be easily localized. The results show that the ER/FF ratio is higher for the n-poor system compared to n-rich one.

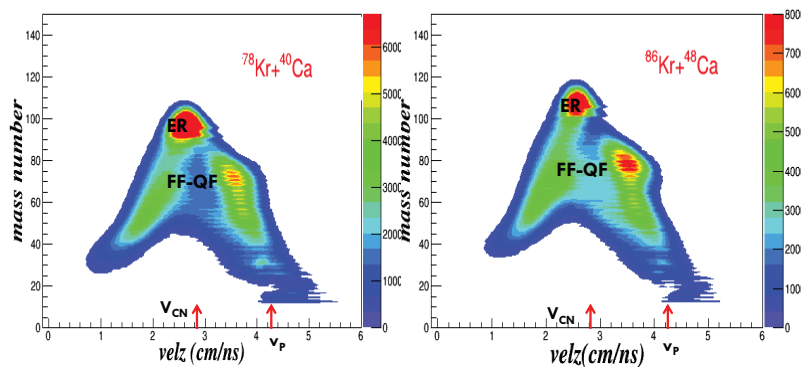


Figure 12 Mass vs parallel velocity for the two systems.

4 Conclusions

Results of the study of the $^{78,86}\text{Kr}+^{40,48}\text{Ca}$ reactions at 10 AMeV incident energy are presented. Kinematical characteristics of the IMF seem to indicate an high degree of relaxation of the system formed in the collision before the breakup, as in typical fusion-fission like reaction mechanisms. Staggering effects are evident in the IMF charge distributions, as well as different isotopic composition and neutron enrichment for the reaction products in the two systems. Global feature analyses show differences between the two systems in the contribution arising from the various reaction mechanisms like fusion-fission, quasi-fission and fusion- evaporation.

The observed effects could be due to the role of the N/Z degree of freedom on the decay channels. Data analysis and more refined comparisons with theoretical models are in progress. A Letter of Intent has been presented for an experiment at radioactive ion beam facility SPES at INFN-LNL, with $^{88-94}\text{Kr} + ^{40-48}\text{Ca}$ at

10MeV/A, in order to study these effects in higher N/Z systems and further improve the knowledge in this field.

References

1. G. Ademard et al. Phys. Rev. C 83, 054619 (2011)
2. P.N. Nadtochy et al., Phys. Rev. C 75, 064614 (2007)
3. A. Pagano et al., Nucl. Phys. A734, 504 (2004)
4. G. Politi et al., IEEE Nuclear Science Symposium Conference Record N28, 1140 (2006);
5. M. Alderighi et al., IEEE Trans. Nucl. Sci. 52, 1624 (2005)
6. R. Bassini et al., IEEE Nuclear Science Symposium Conference Record N14, 173 (2006)
7. E. De Filippo, A. Pagano, EPJA681 32 (2014)
8. I. Lombardo et al., Phys. Rev. C 84, 024613 (2011)
9. G. Casini Phys.Rev. C 86, 011602(R) (2012)
10. M. D'Agostino et al., Nucl. Phys. A 861, 47 (2011)
11. Sh.A. Kalandarov, G.G. Adamian, N.V. Antonenko, W. Scheid, Phys. Rev. C 82, 044603 (2010)
12. A.S. Zubov, G.G. Adamian, N.V. Antonenko, S.P. Ivanova, W. Scheid, Phys. Rev. C 68, 014616 (2003)
13. H.Hauser and H.Feshbach, Phys. Rev. 87 366 (1952)
14. L.G.Moretto Phys. Rev. A247, 221 (1975)
15. N.Bohr and J.A.Wheeler, Phys. Rev. 56, 426 (1939)
16. D.J.Hinde et al., Nucl.Phys. A472, 318 (1987)
17. G. Politi et al., EPJ Web of Conferences 21, 02003 (2012)
18. S. Pirrone et al., AIP Conf. Proc. 1524, 7 (2013)